Article:
Ruprecht, C, Bartetzko, MP, Senf, D et al. (8 more authors) (2017) A Synthetic Glycan Microarray Enables Epitope Mapping of Plant Cell Wall Glycan-Directed Antibodies. Plant Physiology, 175 (3). pp. 1094-1104. ISSN 0032-0889

https://doi.org/10.1104/pp.17.00737

Plant Physiology Preview. Published on September 18, 2017, as DOI:10.1104/pp.17.00737

Short title:

Epitope Mapping of Cell Wall-Directed Antibodies

Corresponding author:

Fabian Pfrengle, Department of Biomolecular Systems, Max-Planck-Institute of Colloids and Interfaces, Am Mühlenberg 1, 14476 Potsdam, Germany

Title:

A synthetic glycan microarray enables epitope mapping of plant cell wall glycan-directed antibodies

Authors:

Colin Ruprecht[1], Max P. Bartetzko[1,2], Deborah Senf[1,2], Pietro Dallabernadina[1,2], Irene Boos[3], Mathias C. F. Andersen[3], Toshihisa Kotake[4], J. Paul Knox[5], Michael G. Hahn[6], Mads H. Clausen[3], Fabian Pfrengle[1,2*]

Affiliations:

[1]Department of Biomolecular Systems, Max-Planck-Institute of Colloids and Interfaces, Am Mühlenberg 1, 14476 Potsdam, Germany
[2]Institute of Chemistry and Biochemistry, Freie Universität Berlin, Arnimallee 22, 14195 Berlin, Germany
[3]Department of Chemistry, Technical University of Denmark, Kemitorvet, Building 207, 2800 Kgs. Lyngby, Denmark
[4]Graduate School of Science and Engineering, Saitama University, 255 Shimo-okubo, Sakura-ku, Saitama 338-8570, Japan
[5]Centre for Plant Sciences, Faculty of Biological Sciences, University of Leeds, Leeds LS2 9JT. UK
[6]Complex Carbohydrate Research Center, University of Georgia, 315 Riverbend Road, Athens, GA 30602-4712, USA

One sentence summary:
Determining exact epitopes for cell wall-directed monoclonal antibodies provides the basis for a detailed elucidation of polysaccharide structures at the cellular level.

Author contributions:

C.R. and F.P. designed the research and drafted the manuscript. C.R. performed experiments and analyzed the data. M.P.B., D.S., P.D., M.C.F.A., and I.B. synthesized the glycans. F.P. and M.H.C. supervised the chemical synthesis. M.G.H., J.P.K., and T.K. provided antibodies and enzymes. All authors contributed to and approved the final version of the manuscript.

Corresponding author: Fabian.Pfrengle@mpikg.mpg.de

Abstract

In the last three decades, more than 200 monoclonal antibodies have been raised against most classes of plant cell wall polysaccharides by different laboratories world-wide. These antibodies are widely used to identify differences in plant cell wall components in mutants, organ and tissue types, and developmental stages. Despite their importance and broad use, the precise binding epitope for only a few of these antibodies has been determined. Here, we use a plant glycan microarray equipped with 88 synthetic oligosaccharides to comprehensively map the epitopes of plant cell wall glycan-directed antibodies. Our results reveal the binding epitopes for 78 arabinogalactan-, rhamnogalacturonan-, xylan-, and xyloglucan-directed antibodies. We demonstrate that, with knowledge of the exact epitopes recognized by individual antibodies, specific glycosyl hydrolases can be implemented into immunological cell wall analyses, providing a framework to obtain structural information on plant cell wall glycans with unprecedented molecular precision.

Introduction

Plant cell walls are highly complex sophisticated composites largely comprised of polysaccharide networks with essential functions in the life cycle of plants. Plant physiology, growth, and development all depend on the structure and dynamics of the cell wall (Keegstra 2010). Moreover, cell wall polysaccharides receive an enormous interest as sources of renewable materials and for the production of biofuels (Pauly and Keegstra 2010). To enhance the economic viability of biomass as a renewable resource, an increasing number of genetically engineered plants with modified cell wall compositions have been generated (Loque, Scheller, and Pauly 2015). However, a prerequisite to performing targeted genetic modifications is a detailed knowledge of plant cell wall structure and its biosynthesis.

To characterize these very diverse plant cell wall components and the genes responsible for their synthesis, biochemical tools are required that can identify molecular structures in the cell wall with high precision. Glycosidic linkage analyses of cell wall extracts can provide quantitative information on the abundance of monosaccharides and their linkage types (Pettolino et al. 2012). This information can then be used to derive occurrence and structure of different polysaccharide classes. However, this method can only be applied to whole organs, and thus it remains unclear which tissue and cell types contain the identified polysaccharides. To obtain high spatial resolution, a large number of monoclonal antibodies (mAbs) that bind distinct classes of cell wall polysaccharides have been developed (Pattathil et al. 2010; Classen et al. 2004; McCartney, Marcus, and Knox 2005; Meikle et al. 1994; Ralet et al. 2010; Willats, Marcus, and Knox 1998). These mAbs are widely used to localize polysaccharides in cells and tissues of various plant species (Guillon et al. 2004; Classen et al. 2004; da Costa et al. 2017), and to characterize mutant plants with alterations in cell wall composition (Pacheco-Villalobos et al. 2016; Gendre et al. 2013). Yet, the limited information on the precise molecular structures bound by the mAbs has hindered a comprehensive interpretation of immunological cell wall analyses.

Due to the heterogeneity and diversity of glycoforms within polysaccharide classes, the small number of well characterized mAbs have the precision with which these molecular probes can

be used to infer polysaccharide occurrence or abundance. The only viable option to precisely determine the binding epitopes of large numbers of the existing mAbs is to screen their binding capabilities with structurally well-defined oligosaccharides. Previous studies with cell wall-related oligosaccharides have demonstrated that glycan microarrays (Rillahan and Paulson 2011) can be used to determine the binding epitopes of cell wall glycan-directed mAbs (Pedersen et al. 2012; Schmidt et al. 2015). Synthetic chemistry is ideally suited to procure these well-defined oligosaccharides as it provides *de novo* designed oligosaccharides of exceptional purity. Herein, we report the production of a microarray equipped with 88 synthetic oligosaccharides that enabled us to determine the binding epitopes of 78 plant cell wall glycan-directed mAbs. We further show that glycosyl hydrolases can be used on plant sections to specifically modify cell wall polysaccharides, generating new glycan epitopes that are detectable by specific mAbs. Integrating glycosyl hydrolases in immunological cell wall analyses thus provides additional structural information on plant cell wall polysaccharides.

Results and Discussion

Generation of a synthetic plant glycan microarray and determination of mAb epitopes

We have chemically synthesized a library of plant cell wall derived oligosaccharides either using automated glycan assembly (compounds 1-66, Figure 1A) (Bartetzko et al. 2015; Bartetzko et al. 2017; Dallabernardina et al. 2016, 2017; Schmidt et al. 2015; Senf et al. 2017) or by conventional solution-phase chemistry (compounds 67-88, Figure 1A) (Andersen, Boos, et al. 2016; Andersen, Kracun, et al. 2016; Zakharova, Madsen, and Clausen 2013; Andersen 2014). These include the following oligosaccharides; xylan oligosaccharides (compounds 1-22) composed of a β-1,4-linked xylan backbone with arabinofuranose substitutions in the 2- and/or 3-position of the xylose residues or with glucuronic acid substitutions in the 2-position; glucan oligosaccharides (compounds 23-39) with a β-1,4-linked glucan backbone that can be substituted with α-1,6-linked xylose residues (xyloglucan, compounds 25-32) or interspersed with β-1,3-linkages (mixed-linkage glucans, MLGs, compounds 33-39); pectin derived oligosaccharides including β-1,4-linked type I (arabino-)galactans (compounds 40-49, 67-77, 86-88) and a rhamnogalacturonan-I (RG-I) backbone oligosaccharide (compound 78); type II (arabino-)galactan oligosaccharides composed of a β-1,3-linked backbone branched with β-1,6-linked galactan side chains that can be further substituted with α-1,3-linked arabinofuranoses or a terminal β-1,6-linked glucuronic acid (compounds 50-66, 79-85).

The synthetic oligosaccharides were printed at four different concentrations on chemically activated glass slides using a non-contact piezoelectric microarray printer (Figure 1). This glycan array platform was used to systematically map the epitopes of 209 plant cell wall glycan-directed mAbs that were obtained from different laboratories. The binding strength of the mAbs to the printed oligosaccharides correlates with the fluorescence intensity observed for an individual interaction (Figure 1B, Supplementary Data File 1). To define a positive signal we required at least a 4-fold increase of signal intensity over background and a value of at least 4% of the maximal value for a particular antibody. The quantification of the binding strength of the xylan-directed mAb LM10 for the four different glycan printing concentrations is depicted in Figure 1C.

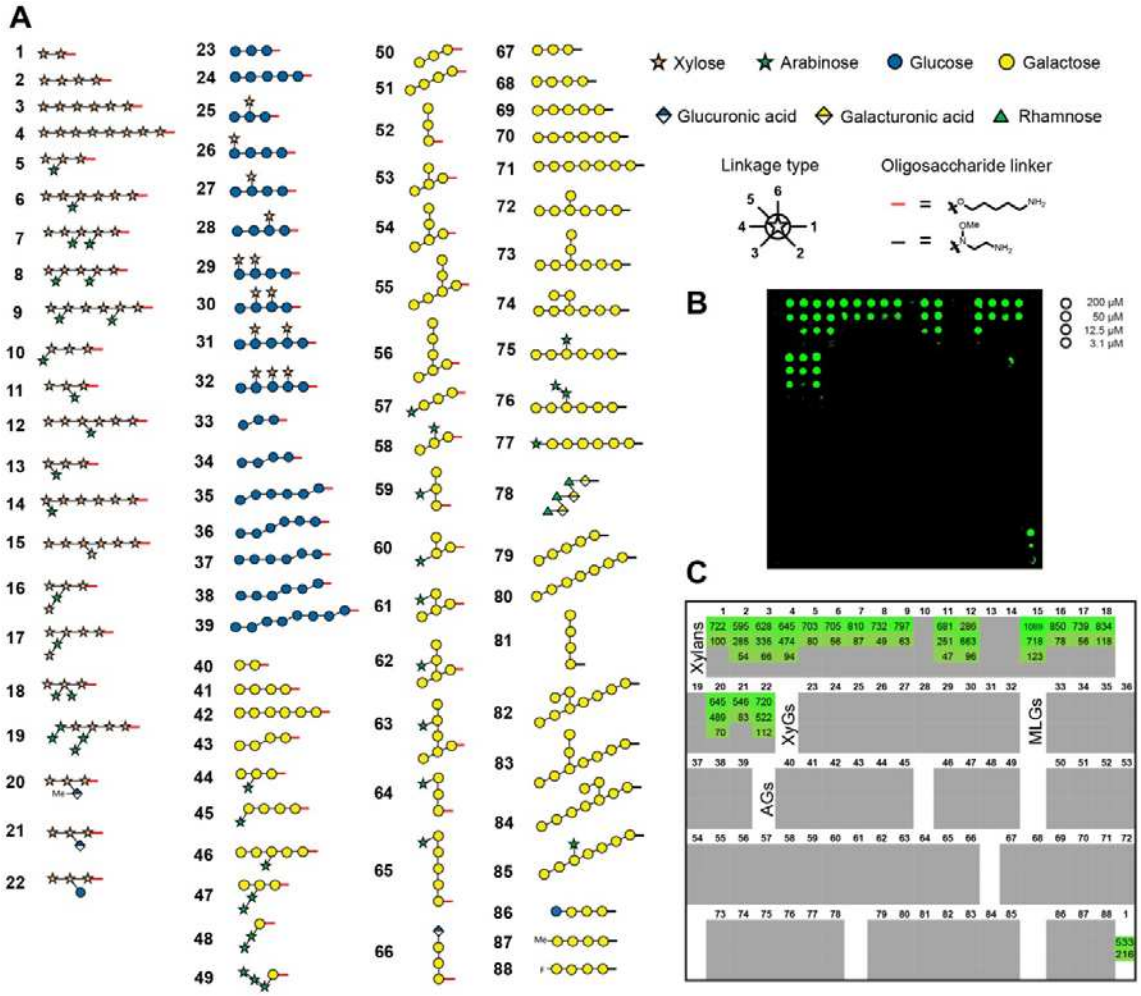

Figure 1. A glycan microarray equipped with synthetic cell wall oligosaccharides.

(**A**) The printed oligosaccharides comprise fragments of four major polysaccharide classes: xylans (compounds 1-22), glucans (23-39), galactans (40-77, 79-88), and rhamnogalacturonan-I (78). Red and black bars at the reducing end of the oligosaccharides indicate the different linkers of the respective compounds produced either by automated glycan assembly (1-66) or conventional solution-phase chemistry (67-88). The legend for linkage types denotes at which position the next monosaccharide is attached. (**B**) Fluorescence signal for binding of LM10 to xylan oligosaccharides. Each compound was printed at four different concentrations as indicated on the right. The printing pattern of the glycan microarray is depicted in C. (**C**) Quantification of the fluorescence signal for LM10. The values denote fold-change over background. Only signals of more than 4-fold above background and above 4% of the maximal value are shown. Note that the 200µM and the 50µM concentrations of oligosaccharide 1 were reprinted on the array as the last spots (lower right corner) to confirm constant printing efficiency.

We created a summarizing heatmap of the binding capabilities of individual mAbs and the 88 different synthetic glycans (Figure 2A). Based on the binding patterns of the mAbs, we aimed to identify a common motif among the recognized oligosaccharides that represents the actual epitope. Several antibodies whose epitopes had been characterized in detail previously using defined oligosaccharides (Andersen, Boos, et al. 2016; Puhlmann et al. 1994; Willats, Marcus,

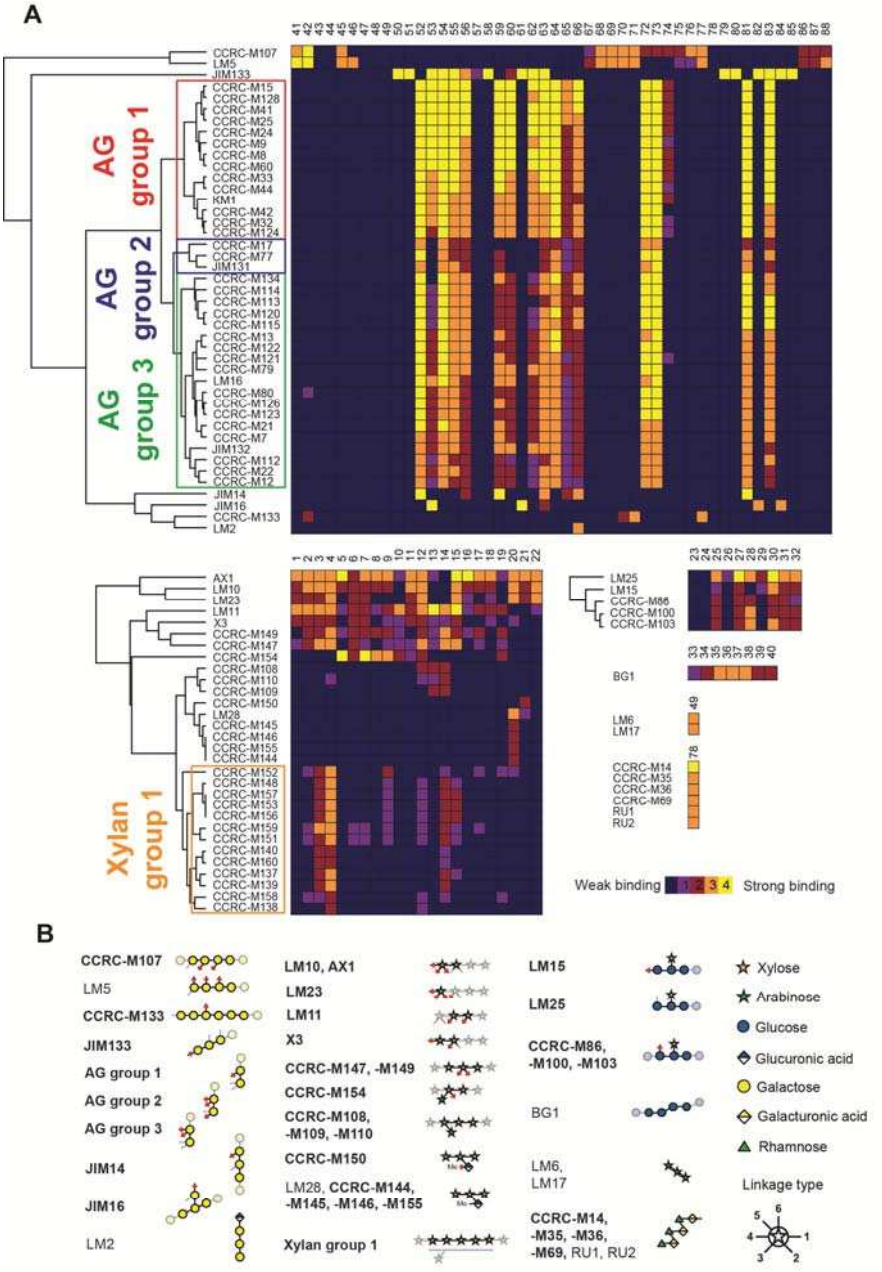

Figure 2. Identification of plant cell wall mAb epitopes.

(**A**) Heatmaps of the binding interactions between individual mAbs and respective synthetic glycans. The binding strength of an antibody to a compound is visualized by a color code (0-4) which denotes how many of the four printed glycan concentrations displayed a positive fluorescence signal. Antibodies were grouped based on hierarchical clustering. The representative result of three replicates is shown. The full heatmap is shown in Supplementary Figure 1. (**B**) Identified epitopes of cell wall-directed antibodies. Linkages that are marked with a red bar indicate positions that must not be occupied. Light linkages and light monosaccharide symbols indicate positions for substitutions that are allowed but not required for binding. For antibodies depicted in bold, no or very limited epitope information was available previously. Note that mAbs of xylan group 1 tolerate different degrees of low-level substitution of the xylan backbone.

and Knox 1998; Steffan et al. 1995) were included in our analysis. We were able to confirm the specificity of these mAbs, for example the binding of LM2 to glucuronic acid that is terminally attached to 1,6-linked galactan (Smallwood et al. 1996), and of LM6 and LM17 to 1,5-linked arabinan (Verhertbruggen et al. 2009) (Figure 2B). Using the binding patterns of previously uncharacterized antibodies, we identified the binding epitopes for an additional 78

mAbs (Figure 2B). To resolve similarities in the binding specificities of the mAbs, we used hierarchical clustering on the data obtained with arabinogalactan- (AG), xylan-, and xyloglucan-binding antibodies.

Arabinogalactan-directed antibodies

The hierarchical clustering identified three large groups of AG-binding antibodies among the antibodies tested. Based on the oligosaccharides bound we deduced that these three groups of antibodies bind to β-1,6-linked galactans that can be present in type I or type II (arabino-)galactan. None of these antibodies bind to exclusively β-1,3-linked or β-1,4-linked galactans (Figure 2, Supplementary Figure 2A-C). This observation is consistent with previous ELISA experiments that revealed binding of these mAbs to diverse classes of polysaccharides, indicating the existence of these β-1,6-linked galactan epitopes in rhamnogalacturonan I, type II AG, and other pectic polysaccharide preparations from various plant sources (Pattathil et al. 2010).

While the binding pattern of these mAbs for the tested arabinogalactan oligosaccharides is largely similar, a major difference between these groups is their binding properties to oligosaccharides 53, 60, and 62. AG group 1 antibodies bind strongly, AG group 3 antibodies bind weakly, and AG group 2 antibodies do not bind to these oligosaccharides at all (Figure 2A, Supplementary Figure 2A-C). In these three oligosaccharides the "lower" galactose of a β-1,6-linked galactan disaccharide epitope is substituted in the 3-position either with galactose or with arabinose. The antibody groups may be further distinguished based on their binding to oligosaccharide 74. The AG group 1 antibodies bind to oligosaccharide 74, while AG groups 2 and 3 do not. In oligosaccharide 74, the "upper" galactose residue of a β-1,6-linked galactan disaccharide epitope is substituted at the C4-position. Based on the oligosaccharides tested, we conclude that AG group 2 antibodies bind to a minimal epitope of a β-1,6-linked disaccharide and the "lower" galactose may be part of a β-1,4-linked galactan backbone. The minimal epitope for the AG group 1 and 3 antibodies cannot be delineated completely with the oligosaccharides tested, although it appears that AG group 1 and 3 antibodies bind to a β-1,6-linked disaccharide of which the "lower" galactose can be part of both a β-1,3-linked and β-1,4-linked galactan backbone (as for example in oligosaccharides 53 and 72). Unlike AG group 3 antibodies, AG group 1 antibodies tolerate a substitution at the 4-position on the "upper" galactose.

More differentiated binding patterns to arabinogalactans were observed for antibodies JIM14 and JIM16. The binding pattern JIM14 revealed that at least three consecutive β-1,6-linked galactose units are required for binding (Figure 2A, Supplementary Figure 2D). Arabinose substitution at the central galactose unit did not affect binding, indicating that also arabinosylated galactan polysaccharides can be recognized by JIM14. However, lack of binding to compound 64 showed that the third galactose towards the non-reducing terminus must not be arabinosylated. To investigate if JIM14 binds an internal epitope or the non-reducing end of β-1,6-galactans, we synthesized two glycans that do not permit binding to the terminal galactose unit (compounds 65 and 66). Based on JIM14 binding to compounds 65 and 66, we conclude that JIM14 binds an internal epitope on β-1,6-linked galactans. JIM16 on the other hand recognizes a β-1,3-linked galactan backbone when substituted with a single β-

1,6-linked galactose residue (Figure 2B) as this antibody bound strongly only to compounds 53 and 61 (Figure 2A).

We identified an antibody that specifically recognizes the β-1,3-linked galactan backbone in AGs. JIM133 selectively binds all tested β-1,3-linked galacto-oligosaccharides, with tolerance for various β-1,6-linked arabinose and galactose substitutions. The strongly reduced binding of JIM133 to compound 57 compared to compound 50 indicates that this antibody requires the free non-reducing end of the galactan for binding. JIM133 can thus be used to detect the non-reducing ends of the β-1,3-linked galactan backbone in AG structures of AGPs.

We identified two antibodies in addition to the previously characterized LM5 antibody (Jones, Seymour, and Knox 1997; Andersen, Boos, et al. 2016) that recognize β-1,4-linked type I galactan, a prominent side chain in RG I. CCRC-M107 requires a minimum of DP (degree of polymerization) = 4 (Supplementary Figure 2E, compounds 41, 42, 68-71). In contrast, CCRC-M133 only binds to β-1,4-linked galactan with DP = 6 or greater (Supplementary Figure 2F, compounds 42, 70, 71). Their strong binding to oligosaccharide 77 indicates that CCRC-M107 and CCRC-M133 bind to internal parts of type I galactan. Our results further show that CCRC-M107 tolerates limited arabinose substitution, whereas CCRC-M133 does not bind to any substituted β-1,4-linked galacto-oligosaccharides tested here.

Xylan-directed antibodies

We identified xylan-directed mAbs that cover most epitopes found in natural xylans. Antibodies in xylan group 1 recognize low-substituted xylans, tolerating to varying degrees different patterns of limited arabinose substitution (Figure 2). These mAbs bind strongly to oligosaccharides 3 and 4, indicating that longer stretches of β-1,4 xylan backbone represent the preferred epitope for these antibodies. Weak binding to substituted xylan oligosaccharides was also observed, e.g. oligosaccharides 9, 12, and 15. However, the available oligosaccharides do not permit an exhaustive determination of the tolerated substitution patterns. The xylan group 1 antibodies with the least tolerance for arabinose substitution of the backbone are CCRC-M140, CCRC-M160, CCRC-M137, and CCRC-M139. CCRC-M152 stands out from the xylan 1 group by the observation that this antibody binds more strongly to oligosaccharide 9 than to oligosaccharide 14, which is different from the binding pattern of the remaining xylan group 1 antibodies. Contrary to these xylan group 1 mAbs, we found LM11, CCRC-M147, and CCRC-M149 to bind the β-1,4-linked xylan backbone with a high tolerance for backbone substitution. With slight differences in the binding patterns, most arabinose-substituted xylan oligosaccharides were recognized.

In addition to these mAbs that recognize the xylan backbone, we also identified several mAbs that specifically detect distinct substituents present on xylan polymers, and do not bind to unsubstituted xylan oligosaccharides (compounds 1-4). For example, we found that CCRC-M154 selectively binds to xylan oligosaccharides with an arabinose substitution in the 3-position. However, compound 18 with two arabinose substituents linked to the same xylose residue was not recognized. On the other hand, we found that CCRC-M108, CCRC-M109, and CCRC-M110 specifically bind to xylan oligosaccharides with arabinose in the 2-position (Figure 2). Interestingly, CCRC-M108, CCRC-M109, and CCRC-M110, specific for 2-

substituted arabinoxylans, were all raised against *Phormium tenax* (New Zealand flax) and had been shown to bind exclusively to isolated *Phormium* xylan and not to xylans from other plants in ELISA experiments carried out with polysaccharide ligands (Pattathil et al. 2010). Thus, 2-substituted arabinoxylans might be specific to certain plants, although monosaccharide linkage analyses have previously suggested a broader occurrence of single arabinose substitution in the 2-position of xylans (Izydorczyk and Biliaderis 1995). Furthermore, we confirm binding of LM28 to xylan oligosaccharides substituted with glucuronic acid in the 2-position (Cornuault et al. 2015). While LM28 binds both methylated and unmethylated glucuronic acid side chains, we here identify mAbs that exclusively bind to either unmethylated glucuronic acid [CCRC-M150, a correction of previously published data; (Schmidt et al. 2015)] or 4-*O*-methyl glucuronic acid (CCRC-M144, CCRC-M145, CCRC-M146, CCRC-M155). None of these antibodies bind to the glucose substituted compound 22, demonstrating that the carboxyl group is essential for binding of these mAbs. Since our collection did not contain esterified xylan oligosaccharides, we were not able to detect antibodies that recognize these epitopes. While LM12 binds to ferulated xylans (Pedersen et al. 2012), antibodies specifically recognizing acetylated xylan are yet to be developed.

The most unexpected result was obtained for LM10, as this frequently used antibody was previously thought to bind low or un-substituted xylan (McCartney, Marcus, and Knox 2005). The glycan microarray experiments show that LM10 binds to all xylan oligosaccharides tested except compounds 10, 13, 14, and 19 (Figure 1B, C). These compounds are all substituted with arabinose either at the 2- or 3-position of the terminal xylose residue. While a lack of binding to compounds 10, 13, and 19 could still be explained by their relatively high arabinose content, absence of binding to compound 14, which was specifically designed to characterize this antibody, unequivocally established that LM10 binds to the non-reducing end of xylans. Similar results were obtained for AX1, X3, and LM23 which also bind to terminal xylose residues but tolerate slightly different substitution patterns.

Intriguingly, all antibodies that bind the non-reducing end were raised against short oligosaccharides as immunogens, except for JIM133. All mAbs that were raised against polysaccharide antigens (72 of 78 mAbs) recognized an internal epitope within the polymer. These observations have important implications for the choice of oligosaccharide antigens to be used for the generation of new cell wall directed antibodies. Instead of internal sequences of complex polymers such as rhamnogalacturonan II, rather terminal oligosaccharides should be used as immunogens.

Xyloglucan-directed antibodies

Many mAbs have been raised against xyloglucan using either oligosaccharides (e.g. LM15 and LM25 (Pedersen et al. 2012; Marcus et al. 2008) or polysaccharides (e.g. CCRC-M86, CCRC-M100, CCRC-M103) as antigens (Pattathil et al. 2010). The majority of these mAbs did not bind to any of our compounds (Supplementary Data File 1), probably because these antibodies require galactose or fucose substitutions for binding which are not included in our xyloglucan oligosaccharide library. Here, we could determine the epitopes for five xyloglucan antibodies. These xyloglucan-directed antibodies recognize a xyloglucan epitope with at least one α-1,6-linked xylose residue linked to a β-1,4-linked glucan backbone (no binding to

unsubstituted β-1,4-linked glucan oligosaccharides 23 and 24 was observed, see Figure 2). While we could not derive whether LM25 binds to terminal or internal parts of xyloglucan, this distinction was possible for LM15 and CCRC-M103 (similarly CCRC-M86 and CCRC-M100). We observed similar binding patterns for these antibodies except for the fact that LM15 does not bind to compound 28, whereas CCRC-M103 does not bind to compound 29 (Figure 2A, Supplementary Figure 2G, H). Compound 28 is an elongated version of compound 25 with one additional glucose unit at the non-reducing end. This additional glucose abolished binding of LM15, suggesting that LM15 only tolerates a single unsubstituted backbone glucosyl residue at the non-reducing end of the oligosaccharide. Based on the importance of the non-reducing end of the oligosaccharides (25 vs 28) for binding we conclude that LM15 is directed towards the non-reducing end, with the requirement for the second last glucose to be substituted with an α-1,6-linked xylose. Contrary to LM15, CCRC-M103 binds more strongly to compound 28 compared to compound 25, suggesting that CCRC-M103 probably binds to internal parts of xyloglucan. The binding of CCRC-M103 to compounds 25, 27, 28, and 30-32 and the lack of binding to compounds 26 and 29 further suggest that CCRC-M103 requires a free glucose at the position next to the xylose substituent towards the non-reducing end.

Rhamnogalacturonan I-directed antibodies

Six antibodies directed at the backbone of RG-I were detected (Figure 2). For antibodies CCRC-M14, CCRC-M35, CCRC-M36, and CCRC-M69, indirect evidence suggested that they bind the backbone of RG-I (Pattathil et al. 2010), but definitive proof was missing. In addition, we could confirm the previously published binding epitope for INRA-RU1 and INRA-RU2, which was determined using purified rhamnogalacturonan oligosaccharides in competitive ELISA experiments (Ralet et al. 2010).

Glycosyl hydrolase digests on the glycan microarray

Next, we investigated if the immobilized glycans can be modified on the array using carbohydrate-active enzymes. Incubation of the microarray slides with arabinofuranosidases acting on arabinoxylan results in de-arabinosylation of the xylan oligosaccharides, as detected with xylan-directed mAbs LM10, CCRC-M154, and the xylan group 1 antibody CCRC-M148 (Figure 3A, B). As expected, CCRC-M148 now recognized oligosaccharides that were previously too heavily arabinosylated to permit binding of this antibody. For example, oligosaccharide 8 was bound after de-arabinosylation (Figure 3 A, B), suggesting that CCRC-M148 binds to unsubstituted xylan backbones of DP = 5 or greater, a refinement of previous characterization data for this antibody which indicated CCRC-M148 binding to xylan oligosaccharides of DP = 6 or greater (Schmidt et al. 2015). The binding of CCRC-M154, which is selective for 3-substituted arabinofuranoses, was strongly reduced after arabinofuranosidase treatment. Restoration of LM10 binding to oligosaccharides with an arabinose attached to the non-reducing xylose unit (compounds 10, 13, and 14) upon de-arabinosylation further confirmed the proposed binding mode of LM10 directed at the non-reducing end of xylans.

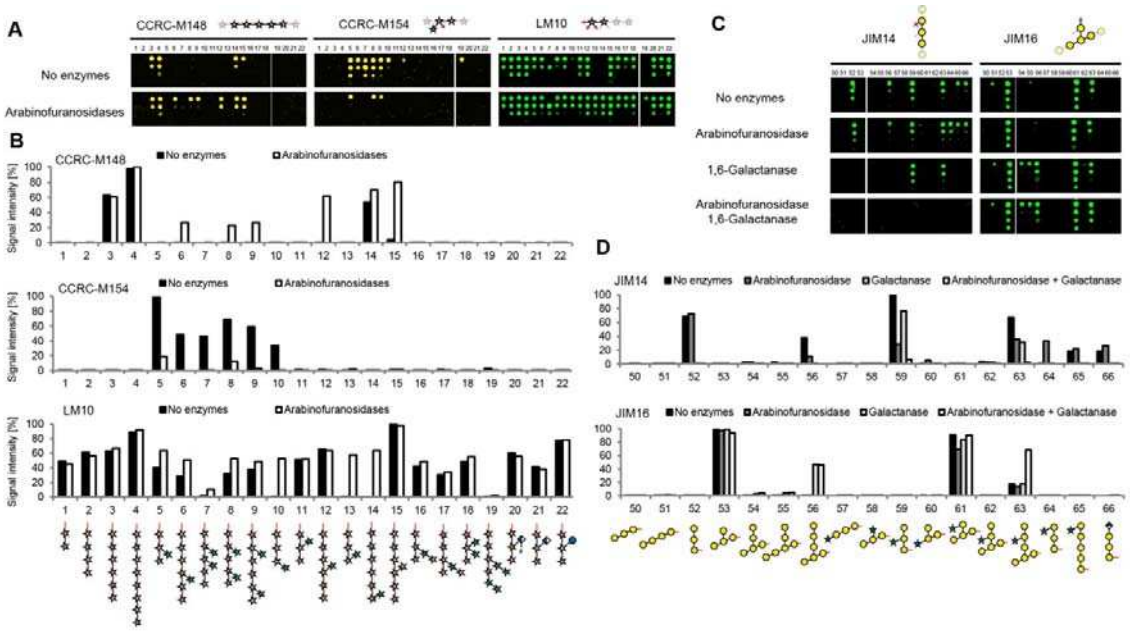

Figure 3. The glycan microarray as a platform to characterize glycosyl hydrolases.

(**A**) "On-array" treatment of xylan oligosaccharides with arabinofuranosidases and assessment of arabinose cleavage with CCRC-M148, CCRC-M154, and LM10. Note that the 200 µM concentration for oligosaccharide 7 was misprinted, resulting in a low signal intensity after quantification (see LM10). (**B**) Quantification of the fluorescence signal with and without arabinofuranosidase treatment as shown in A. (**C**) Arabinogalactan digest on the array with 1,6-galactanase and arabinofuranosidase detected with JIM14 and JIM16. (**D**) Quantification of the fluorescence signals in C. Representative results of three independent experiments are shown.

As a second example, we used a β-1,6-endogalactanase (Kitazawa et al. 2013; Kotake et al. 2004) to trim the side chains of synthetic AG oligosaccharides. This endogalactanase was reported to hydrolyze β-1,6-linked galactan side chains of AGP polysaccharides until one or two galactose residues remain on the β-1,3-linked galactan backbone (Kitazawa et al. 2013). Binding of JIM14, which recognizes glycans with at least three consecutive β-1,6-linked galactose residues (Figure 2B), was abolished upon treatment with β-1,6-endogalactanase for all synthetic galactan oligosaccharides that were not substituted with arabinose at the central galactose unit (oligosaccharides 52, 56, 65 and 66), but not for the oligosaccharides that were arabinosylated (59 and 63, Figure 3C, D). To remove the arabinoses from oligosaccharides 59 and 63, we used an arabinofuranosidase and unexpectedly found slightly reduced binding of JIM14 to oligosaccharides 56, 59, and 63, probably due to traces of galactanase activity in the enzyme preparation. However, when both arabinofuranosidase and galactanase were applied together on the glycan microarray, recognition of oligosaccharides 59 and 63 was completely abolished (Figure 3C, D). This indicated that the galactanase only tolerates arabinose substitution in certain positions of the galactan to be hydrolyzed. JIM16 recognizes the 1,3-linked galactan backbone when substituted with a single 1,6-linked galactose residue (Figure 2B). Binding of JIM16 to oligosaccharide 56 after galactanase digestion and oligosaccharide 63 after arabinofuranosidase and galactanase digestion confirmed that a single 1,6-linked galactose unit remained on the 1,3-linked backbone of these oligosaccharides (Figure 3D). Although exact substrate specificities of glycosyl hydrolases acting on cell wall glycans can only be determined by structural characterization of the reaction products after incubation of

oligo- or polysaccharides, these data demonstrate that the synthetic plant glycan microarray platform provides a useful tool, in combination with well-characterized mAbs, to collect valuable information on the substrate specificities of glycosyl hydrolases in a high-throughput fashion. As our platform provides specific information on the enzyme's substrate specificities, it represents a powerful extension of previous polysaccharide-based array platforms for the identification of new glycosyl hydrolases (Vidal-Melgosa et al. 2015; Walker et al. 2017).

Implementation of glycosyl hydrolases into cell wall labeling studies

Specific knowledge of the molecular structure bound by a particular mAb and the substrate specificities of glycosyl hydrolases acting on the very same polysaccharide allows for a detailed immunological elucidation of glycan structures in the cell wall. We performed antibody staining of xylans and AGs in roots of *Brachypodium distachyon* (Brachypodium), which is a model system to study grass roots (Hardtke and Pacheco-Villalobos 2015). We used CCRC-M148 to detect unsubstituted xylan stretches, CCRC-M154 to identify arabinosylated xylan, and LM10 to specifically track the non-reducing ends of xylan polymers (Figure 4). Interestingly, these three mAbs showed distinct binding patterns on sections of the root elongation zone. CCRC-M148 bound to walls of all cells of the stele (central metaxylem to pericycle cells), CCRC-M154 bound to walls of cells in the stele and in the surrounding cortex, and LM10 selectively bound to walls of pericycle and metaxylem cells. Thus, the secondary cell walls in the stele contain xylans with a low degree of arabinosylation, whereas the primary walls in cortex cells contain only highly arabinosylated xylans (Christensen et al. 2010). To confirm that the binding of CCRC-M154 to the cortex cells results from their high arabinoxylan content, we applied arabinoxylan-specific arabinofuranosidases (McCleary et al. 2015) to the sections prior to antibody staining. Indeed, CCRC-M154 binding was completely abolished in all cell walls, while CCRC-M148 now also bound to the cortex cell walls in addition to the stele walls. Apparently, de-arabinosylating the xylan exposed unsubstituted xylan stretches for CCRC-M148 binding in cortex cell walls. LM10 binding was not affected by arabinofuranosidase treatment, suggesting that arabinosylation of the terminal xylose unit of the xylan chain was not causative for the observed differential binding of LM10 to the walls of different cell types. Instead, we hypothesize that the non-reducing ends of the xylan chains are covalently modified or covered by interactions with other components of the cell wall matrix.

JIM14 and JIM16 represent an interesting pair of antibodies to visualize differentially branched galactan in type II AG-polysaccharides that are present on arabinogalactan proteins (AGPs; Figure 4). Yariv stain-based localization of AGPs showed that all cells in the root sections contained AGPs in their cell wall (Supplementary Figure 3). Lack of JIM16 binding to these root sections suggests that the AG-structures contain no single β-1,6-linked galactose substitutions of the backbone but rather longer galactan side branches. However, only metaphloem cells were stained by JIM14. We hypothesized that all other cells might display higher degrees of arabinosylation than recognizable by JIM14. To test this hypothesis, we incubated the sections with arabinofuranosidase prior to antibody staining. Indeed, de-arabinosylation resulted in JIM14 binding to all cells. As we were able to convert the JIM14 epitope into the JIM16 epitope by enzymatically trimming the β-1,6-linked galactan side chains on the microarray (Figure 3C, D), we tested if the JIM16 epitope could be revealed in

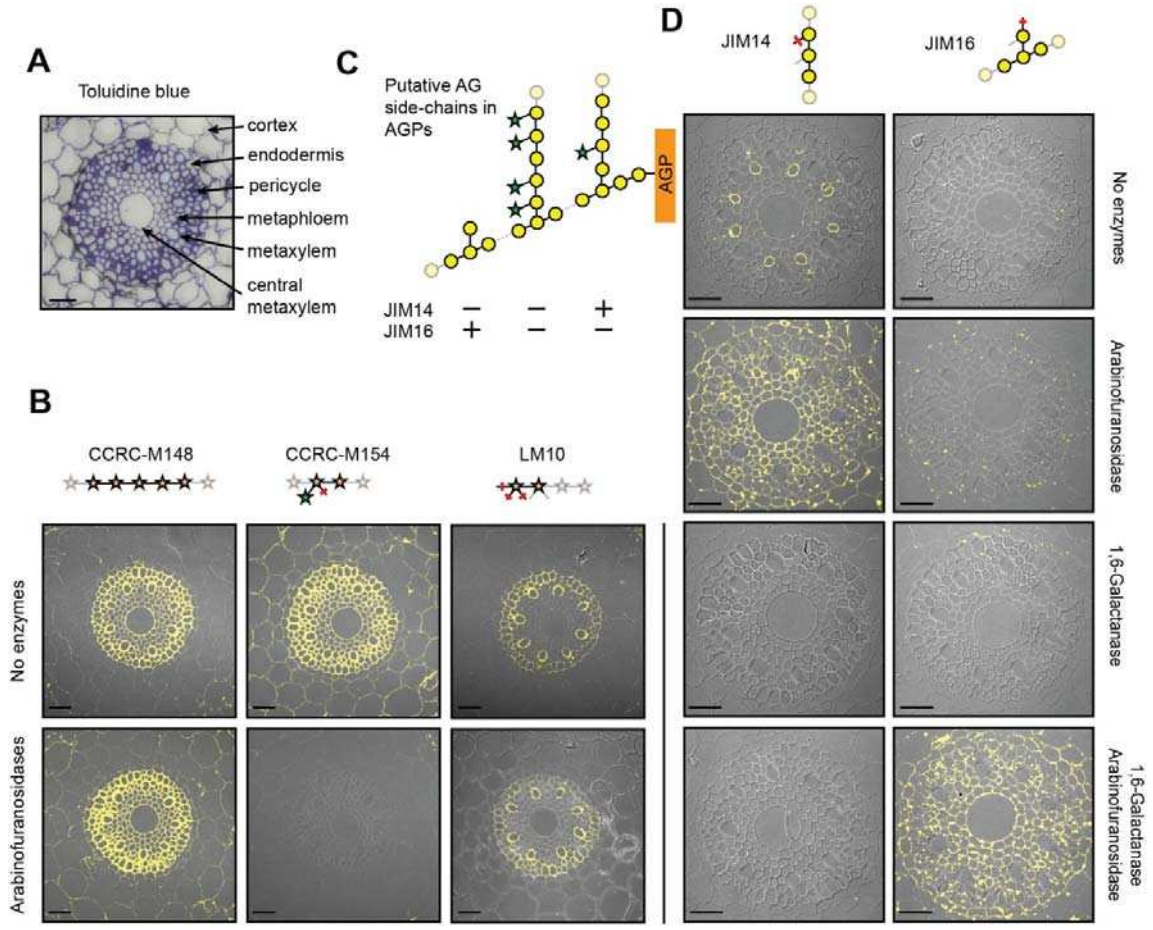

Figure 4. Immunological analyses reveal detailed molecular glycan structures in Brachypodium root sections

(**A**) Toluidine blue was used to stain sections and identify cell types (Hardtke and Pacheco-Villalobos 2015). (**B**) Immunolabelling of (arabino)xylan using CCRC-M148, CCRC-M154, and LM10 in root tips of Brachypodium. (**C**) Putative arabinogalactan (AG) side chains with expected binding of JIM14 and JIM16. (**D**) Immunolabelling of AG-structures using JIM14 and JIM16. Arabinofuranosidases and galactanases were incubated on the sections prior to the antibody staining to reveal xylan and galactan epitopes. The scale bars indicate 50 µm. Representative results of three independent biological replicates are shown.

the root sections as well. We incubated the sections with the β-1,6-galactanase that was used on the microarray, but did not observe any JIM16 binding upon subsequent antibody staining. Only when both arabinofuranosidase and β-1,6-galactanase were applied together prior to antibody staining was the JIM16 epitope revealed in all root cells. Apparently, the metaphloem cells contain at least some arabinose substitution, which inhibited complete enzymatic cleavage of the β-1,6-linked galactan branches. Thus, we conclude that the AG-structures in metaphloem cells contain a low degree of arabinosylation, whereas all other root cells display highly arabinosylated AGPs. The complexity of the AG-structure in AGPs has previously been associated with growth phenotypes in Brachypodium mutants and an Arabidopsis mutant (Knoch et al. 2013; Pacheco-Villalobos et al. 2016). Both studies used glycosidic linkage analyses on whole roots or root segments to show differences in type II AG related galactose linkages (Knoch et al. 2013; Pacheco-Villalobos et al. 2016). To resolve

which cell types display the differences in AGP complexity, more detailed analyses are now feasible based on the newly derived epitope information for type II AG-specific antibodies and the possibility for integrating specific glycosyl hydrolases into cell wall analyses.

It is important to note that integrating glycosyl hydrolases to specifically reveal antibody epitopes is different to previous studies, in which plant sections were pre-treated with a pectate lyase (Herve et al. 2009; Marcus et al. 2008; Marcus et al. 2010) to unmask xylan, xyloglucan, and mannan epitopes (Herve et al. 2009; Marcus et al. 2008; Marcus et al. 2010). The rational use of glycosyl hydrolases to alter the molecular structure of specific cell wall glycans provides additional structural information on the respective glycan. As this approach is limited by the availability of glycosyl hydrolases and antibodies with precisely known specificities, further expansion of the repertoire of suitable enzymes and antibodies will be crucial. This is particularly important as we cannot fully rule out the possibility that, in cases where glycosyl hydrolases with broader substrate specificities are used, multiple cell wall glycans may be affected, and this may lead to masking or de-masking of epitopes.

Conclusions

Using a synthetic plant carbohydrate microarray, we determined the binding epitopes for a large number of plant cell wall glycan-directed mAbs, providing the required information for the specific detection of many complex molecular structures in plant cell wall polysaccharides. We further demonstrate that integrating specific glycosyl hydrolases with immunolabeling studies of cell walls enables an even more comprehensive analysis of distribution patterns of cell wall glycans in plant cells. Our integrated mAb-based analyses provided detailed information on glycan structures in roots of the important model grass species *Brachypodium distachyon*, highlighting the importance of structural understanding of epitopes for the comprehensive interpretation of *in situ* cell wall labeling studies.

Methods

Chemical synthesis of oligosaccharides

Compounds 1-66 were prepared by automated glycan assembly following previously published protocols (Bartetzko et al. 2015; Bartetzko et al. 2017; Dallabernardina et al. 2016, 2017; Schmidt et al. 2015; Senf et al. 2017). Briefly, using an automated synthesizer suitably protected monosaccharide building blocks were added in iterative glycosylation and deprotection cycles to a linker-functionalized Merrifield resin. After assembly was complete, the linker was cleaved and the oligosaccharides were globally deprotected to yield the desired glycans after HPLC-purification. Compounds 67-88 were prepared by conventional solution-phase synthesis (Andersen, Boos, et al. 2016; Andersen, Kracun, et al. 2016; Zakharova, Madsen, and Clausen 2013; Andersen 2014).

Glycan microarray printing

The oligosaccharides were printed on CodeLink *N*-hydroxyl succinimide (NHS) ester-activated glass slides (SurModics Inc., Eden Prairie, MN, USA) using a non-contact piezoelectric spotting device (S3; Scienion, Berlin, Germany). The printing was performed at room temperature and 40% humidity. To ensure constant printing efficiency, the first compound (oligosaccharide 1) was reprinted at the end of the printing run. To assess the binding strength of the antibodies, we diluted the oligosaccharides to four different printing concentrations (200 μM, 50 μM, 12.5 μM, and 3.1 μM) in the coupling buffer (80% (v/v) 50 mM sodium phosphate, pH 8.5, 0.005% (v/v) CHAPS, 20% (w/v) PEG400 (Roth)). After printing, the microarray slides were quenched for 1 h at room temperature in 100 mM ethanolamine, 50 mM sodium phosphate, pH 9, and washed three times with deionized water.

Determining mAb epitopes

We obtained mAbs from different sources as indicated in Supplementary Data File 1, i.e. the Complex Carbohydrate Research Center (CCRC), University of Leeds, the INRA in Nantes, the Classen lab at the University of Kiel, and the University of Melbourne. To incubate 16 different antibodies per microarray slide we applied a FlexWell 16 grid (Grace Bio-Labs, Bend, OR, USA) to the slide. The slides were blocked with 1% (w/v) bovine serum albumin (BSA) in phosphate-buffered saline (PBS) for 1 h at room temperature. Then, hybridoma supernatants containing the antibodies were diluted 1:10 in PBS containing 1% (w/v) BSA and incubated for 1 h on the slides. After three washes with PBS, the slides were incubated with the respective secondary antibodies for 1 h (goat anti-rat IgG AF555 and goat anti-mouse IgM/IgG AF488, Invitrogen, Carlsbad, CA, USA). Unbound secondary antibodies were removed using consecutive washes with 0.1% (v/v) Tween-20 in PBS, PBS, and deionized water. After drying the slides by centrifugation (300 x g, 2 min), the fluorescent signal on the slides was scanned with a GenePix 4300A microarray scanner (Molecular Devices, Sunnyvale, CA, USA). Image analysis and quantification of the fluorescent signal was carried out with the GenePix Pro 7 software (Molecular Devices) using the same settings for each antibody. Based on the raw data (Supplementary Data File 1), we defined positive signals for each of the four printed glycan concentrations based on two thresholds that we cross-validated using antibody binding to known epitopes: (i) 4-fold increase of fluorescent signal intensity

over background and (ii) a fold-change value of at least 4 % of the maximal value of the respective antibody. The resulting numbers of 0–4 therefore indicate the minimum printing concentrations (0 = no binding, 1 = 200 μM, 2 = 50 μM, 3 = 12.5 μM, and 4 = 3.1 μM) required for binding of an antibody. To group similar antibodies we separately performed hierarchical clustering on AG-, xylan-, and xyloglucan-binding antibodies. To this end, we applied the "hclust" function in R using manhattan distance as a distance measure.

Glycosyl hydrolase digests on glycan microarrays

For the arabinoxylan digests, we used two GH43 arabinofuranosidases from *Bacteroides ovatus* (ABFBO17 and ABFBO25) that were purchased from Megazyme (Bray, Ireland). ABFBO17 removes arabinose substituents linked to the 3-position of double-substituted xylose residues, whereas ABFBO25 cleaves single arabinoses in the C2- and C3-position of xylose (Senf et al. 2017). The enzymes were used at a concentration of 10 U/ml in 100 mM sodium phosphate buffer, pH 6.5. For the AG digests, we used a GH51 arabinofuranosidase from *Aspergillus niger* (AFASE) purchased from Megazyme at a concentration of 0.1 U/ml and an endo-1,6-galactanase from *Trichoderma viride* (Tv6GAL) at a concentration of 5 U/ml, both in sodium citrate buffer, pH 4.5. Tv6GAL was expressed recombinantly in *Pichia pastoris* as previously described (Kotake et al. 2004). In both arabinoxylan and AG digests, the enzymes were applied directly in the 16 well grid of a microarray slide and incubated over night at 37°C. The corresponding buffers without enzymes were used as controls. After washing the slides twice with PBS, blocking and antibody staining were performed as described above. Secondary antibodies used were goat anti-rat IgG AF555 for LM10, JIM14, and JIM16, and goat anti-mouse IgM AF594 for CCRC-M148 and CCRC-M154. The fluorescent signal was recorded with a GenePix 4300A microarray scanner and quantified with the GenePix Pro 7 software.

Immunofluorescence analysis of Brachypodium root sections

To analyze arabinoxylan and AG-structures in Brachypodium roots, we grew Brachypodium (accession Bd21) on vertical MS agar plates under 16 h light/8 h dark cycles. Root tips were harvested four days after germination and fixed for 1 h in a 2.5% (v/v) glutaraldehyde solution. Dehydration and embedding into LR White was performed as previously described (Lee et al. 2012). The root tips were cut into 1 μm sections using a Leica Ultracut UCT ultramicrotome. The antibody staining was performed as described for the glycan microarray experiments using goat anti-rat IgG AF555 for LM10, JIM14, and JIM16, and goat anti-mouse IgM AF594 for CCRC-M148 and CCRC-M154. AGP-localization in the sections was carried out as previously described (Goellner, Gramann, and Classen 2013). In brief, after blocking the sections with BSA-buffer, $(\beta\text{-D-Glc})_3$ Yariv phenylglycoside (βGlcY, 400 μg/mL in 0.15 M NaCl) was applied for 90 min. After three washes with PBS, first a βGlcY-antibody and then the corresponding FITC-labelled anti-rabbit secondary antibody were incubated on the sections. Imaging was carried out with a LSM700 confocal microscope (Zeiss, Jena, Germany). Glycosyl hydrolase digests of arabinoxylan and AG in the sections were performed using the same enzymes and conditions as for the digests on the glycan microarray.

Supplemental Materials

Supplementary Figure 1. Summarizing heatmap of binding interactions between individual mAbs and synthetic glycans.

Supplementary Figure 2. Selected glycan microarray scans.

Supplementary Figure 3. Yariv-based staining of AGPs in Brachypodium root sections and antibody staining negative controls.

Supplementary Data File 1. Quantification of the fluorescence signals (raw data) for all tested antibodies.

Acknowledgements

We gratefully acknowledge financial support from the Max Planck Society, the Fonds der Chemischen Industrie (Liebig Fellowship to F.P.), and the German Research Foundation (DFG, Emmy Noether program PF850/1-1 to F.P.). We thank Andreas Geissner for help with printing the microarrays, Rona Pitschke for technical support, and Dr. Dirk Walther for advice with the hierarchical clustering. We thank Dr. Alexandra Zakharova for the synthesis of oligosaccharide 78. M.H.C. acknowledges financial support from the Carlsberg Foundation, the Danish Strategic Research Council (GlycAct and SET4Future projects), and the Villum Foundation (PLANET project). Provision of anti-βGlcYariv antibody and mAbs KM1 by Dr. Birgit Classen, BG1 by Dr. Wei Zeng, AX1 and X3 by Dr. Fabienne Guillon, and RU1 and RU2 by Dr. Marie Christine Ralet is gratefully acknowledged. Generation of the CCRC series of monoclonal antibodies used in this work was supported by grants from the United States Natural Science Foundation Plant Genome Program (DBI-0421683 and IOS-0923992 to M.G.H.).

Figure legends

Figure 1. A glycan microarray equipped with synthetic cell wall oligosaccharides.

(**A**) The printed oligosaccharides comprise fragments of four major polysaccharide classes: xylans (compounds 1-22), glucans (23-39), galactans (40-77, 79-88), and rhamnogalacturonan-I (78). Red and black bars at the reducing end of the oligosaccharides indicate the different linkers of the respective compounds produced either by automated glycan assembly (1-66) or conventional solution-phase chemistry (67-88). The legend for linkage types denotes at which position the next monosaccharide is attached. (**B**) Fluorescence signal for binding of LM10 to xylan oligosaccharides. Each compound was printed at four different concentrations as indicated on the right. The printing pattern of the glycan microarray is depicted in C. (**C**) Quantification of the fluorescence signal for LM10. The values denote fold-change over background. Only signals of more than 4-fold above background and above 4% of the maximal value are shown. Note that the 200μM and the 50μM concentrations of oligosaccharide 1 were reprinted on the array as the last spots (lower right corner) to confirm constant printing efficiency.

Figure 2. Identification of plant cell wall mAb epitopes.

(**A**) Heatmaps of the binding interactions between individual mAbs and respective synthetic glycans. The binding strength of an antibody to a compound is visualized by a color code (0-4) which denotes how many of the four printed glycan concentrations displayed a positive fluorescence signal. Antibodies were grouped based on hierarchical clustering. The representative result of three replicates is shown. The full heatmap is shown in Supplementary Figure 1. (**B**) Identified epitopes of cell wall-directed antibodies. Linkages that are marked with a red bar indicate positions that must not be occupied. Light linkages and light monosaccharide symbols indicate positions for substitutions that are allowed but not required for binding. For antibodies depicted in bold, no or

very limited epitope information was available previously. Note that mAbs of xylan group 1 tolerate different degrees of low-level substitution of the xylan backbone.

Figure 3. The glycan microarray as a platform to characterize glycosyl hydrolases.

(**A**) "On-array" treatment of xylan oligosaccharides with arabinofuranosidases and assessment of arabinose cleavage with CCRC-M148, CCRC-M154, and LM10. Note that the 200 µM concentration for oligosaccharide 7 was misprinted, resulting in a low signal intensity after quantification (see LM10). (**B**) Quantification of the fluorescence signal with and without arabinofuranosidase treatment as shown in A. (**C**) Arabinogalactan digest on the array with 1,6-galactanase and arabinofuranosidase detected with JIM14 and JIM16. (**D**) Quantification of the fluorescence signals in C. Representative results of three independent experiments are shown.

Figure 4. Immunological analyses reveal detailed molecular glycan structures in Brachypodium root sections

(**A**) Toluidine blue was used to stain sections and identify cell types (Hardtke and Pacheco-Villalobos 2015). (**B**) Immunolabelling of (arabino)xylan using CCRC-M148, CCRC-M154, and LM10 in root tips of Brachypodium. (**C**) Putative arabinogalactan (AG) side chains with expected binding of JIM14 and JIM16. (**D**) Immunolabelling of AG-structures using JIM14 and JIM16. Arabinofuranosidases and galactanases were incubated on the sections prior to the antibody staining to reveal xylan and galactan epitopes. The scale bars indicate 50 µm. Representative results of three independent biological replicates are shown.

Parsed Citations

Andersen, M. C., I. Boos, S. E. Marcus, S. K. Kracun, M. G. Rydahl, W. G. Willats, J. P. Knox, and M. H. Clausen. 2016. 'Characterization of the LM5 pectic galactan epitope with synthetic analogues of beta-1,4-d-galactotetraose', Carbohydr Res, 436: 36-40.

Pubmed: Author and Title
CrossRef: Author and Title
Google Scholar: Author Only Title Only Author and Title

Andersen, M. C. F. & Clausen, M. H. . 2014. 'Synthesis and Application of Plant Cell Wall Oligogalactans', PhD thesis, Technical University of Denmark.

Andersen, M. C., S. K. Kracun, M. G. Rydahl, W. G. Willats, and M. H. Clausen. 2016. 'Synthesis of beta-1,4-Linked Galactan Side-Chains of Rhamnogalacturonan I', Chemistry, 22: 11543-8.

Pubmed: Author and Title
CrossRef: Author and Title
Google Scholar: Author Only Title Only Author and Title

Bartetzko, M. P., F. Schuhmacher, H. S. Hahm, P. H. Seeberger, and F. Pfrengle. 2015. 'Automated Glycan Assembly of Oligosaccharides Related to Arabinogalactan Proteins', Org Lett, 17: 4344-7.

Pubmed: Author and Title
CrossRef: Author and Title
Google Scholar: Author Only Title Only Author and Title

Bartetzko, M. P., F. Schuhmacher, P. H. Seeberger, and F. Pfrengle. 2017. 'Determining Substrate Specificities of beta1,4-Endogalactanases Using Plant Arabinogalactan Oligosaccharides Synthesized by Automated Glycan Assembly', J Org Chem, 82: 1842-50.

Pubmed: Author and Title
CrossRef: Author and Title
Google Scholar: Author Only Title Only Author and Title

Christensen, U., A. Alonso-Simon, H. V. Scheller, W. G. Willats, and J. Harholt. 2010. 'Characterization of the primary cell walls of seedlings of Brachypodium distachyon--a potential model plant for temperate grasses', Phytochemistry, 71: 62-9.

Pubmed: Author and Title
CrossRef: Author and Title
Google Scholar: Author Only Title Only Author and Title

Classen, B., M. Csavas, A. Borbas, T. Dingermann, and I. Zuendorf. 2004. 'Monoclonal antibodies against an arabinogalactan-protein from pressed juice of Echinacea purpurea', Planta Med, 70: 861-5.

Pubmed: Author and Title
CrossRef: Author and Title
Google Scholar: Author Only Title Only Author and Title

Cornuault, V., F. Buffetto, M. G. Rydahl, S. E. Marcus, T. A. Torode, J. Xue, M. J. Crepeau, N. Faria-Blanc, W. G. Willats, P. Dupree, M. C. Ralet, and J. P. Knox. 2015. 'Monoclonal antibodies indicate low-abundance links between heteroxylan and other glycans of plant cell walls', Planta, 242: 1321-34.

Pubmed: Author and Title
CrossRef: Author and Title
Google Scholar: Author Only Title Only Author and Title

da Costa, R. M., S. Pattathil, U. Avci, S. J. Lee, S. P. Hazen, A. Winters, M. G. Hahn, and M. Bosch. 2017. 'A cell wall reference profile for Miscanthus bioenergy crops highlights compositional and structural variations associated with development and organ origin', New Phytol, 213: 1710-25.

Pubmed: Author and Title
CrossRef: Author and Title
Google Scholar: Author Only Title Only Author and Title

Dallabernardina, P., F. Schuhmacher, P. H. Seeberger, and F. Pfrengle. 2016. 'Automated glycan assembly of xyloglucan oligosaccharides', Org Biomol Chem, 14: 309-13.

Pubmed: Author and Title
CrossRef: Author and Title
Google Scholar: Author Only Title Only Author and Title

Dallabernardina, P., Schuhmacher, F., Seeberger, P. H., Pfrengle, F. 2017. 'Mixed-Linkage Glucan Oligosaccharides Produced by Automated Glycan Assembly Serve as Tools To Determine the Substrate Specificity of Lichenase', Chemistry, 13, 3191-3196.

Pubmed: Author and Title
CrossRef: Author and Title
Google Scholar: Author Only Title Only Author and Title

Gendre, D., H. E. McFarlane, E. Johnson, G. Mouille, A. Sjodin, J. Oh, G. Levesque-Tremblay, Y. Watanabe, L. Samuels, and R. P. Bhalerao. 2013. 'Trans-Golgi network localized ECHIDNA/Ypt interacting protein complex is required for the secretion of cell wall polysaccharides in Arabidopsis', Plant Cell, 25: 2633-46.

Pubmed: Author and Title
CrossRef: Author and Title
Google Scholar: Author Only Title Only Author and Title

Goellner, E. M., J. C. Gramann, and B. Classen. 2013. 'Antibodies against Yariv's reagent for immunolocalization of arabinogalactan-proteins in aerial parts of Echinacea purpurea', Planta Med, 79: 175-80.
Pubmed: Author and Title
CrossRef: Author and Title
Google Scholar: Author Only Title Only Author and Title

Guillon, Fabienne, Olivier Tranquet, Laurence Quillien, Jean-Pierre Utille, José Juan Ordaz Ortiz, and L. Saulnier. 2004. 'Generation of polyclonal and monoclonal antibodies against arabinoxylans and their use for immunocytochemical location of arabinoxylans in cell walls of endosperm of wheat', Journal of Cereal Science, 40: 167-82.
Pubmed: Author and Title
CrossRef: Author and Title
Google Scholar: Author Only Title Only Author and Title

Hardtke, Christian S., and David Pacheco-Villalobos. 2015. 'The Brachypodium distachyon Root System: A Tractable Model to Investigate Grass Roots', 18: 245-58.
Pubmed: Author and Title
CrossRef: Author and Title
Google Scholar: Author Only Title Only Author and Title

Herve, C., A. Rogowski, H. J. Gilbert, and J. P. Knox. 2009. 'Enzymatic treatments reveal differential capacities for xylan recognition and degradation in primary and secondary plant cell walls', Plant Journal, 58: 413-22.
Pubmed: Author and Title
CrossRef: Author and Title
Google Scholar: Author Only Title Only Author and Title

Izydorczyk, M. S., and C. G. Biliaderis. 1995. 'Cereal arabinoxylans: Advances in structure and physicochemical properties', Carbohydrate Polymers, 28: 33-48.
Pubmed: Author and Title
CrossRef: Author and Title
Google Scholar: Author Only Title Only Author and Title

Jones, L., G. B. Seymour, and J. P. Knox. 1997. 'Localization of pectic galactan in tomato cell walls using a monoclonal antibody specific to (1->4)-beta-D-galactan', Plant Physiology, 113: 1405-12.
Pubmed: Author and Title
CrossRef: Author and Title
Google Scholar: Author Only Title Only Author and Title

Keegstra, K. 2010. 'Plant cell walls', Plant Physiol, 154: 483-6.
Pubmed: Author and Title
CrossRef: Author and Title
Google Scholar: Author Only Title Only Author and Title

Kitazawa, K., T. Tryfona, Y. Yoshimi, Y. Hayashi, S. Kawauchi, L. Antonov, H. Tanaka, T. Takahashi, S. Kaneko, P. Dupree, Y. Tsumuraya, and T. Kotake. 2013. 'beta-galactosyl Yariv reagent binds to the beta-1,3-galactan of arabinogalactan proteins', Plant Physiol, 161: 1117-26.
Pubmed: Author and Title
CrossRef: Author and Title
Google Scholar: Author Only Title Only Author and Title

Knoch, E., A. Dilokpimol, T. Tryfona, C. P. Poulsen, G. Xiong, J. Harholt, B. L. Petersen, P. Ulvskov, M. Z. Hadi, T. Kotake, Y. Tsumuraya, M. Pauly, P. Dupree, and N. Geshi. 2013. 'A beta-glucuronosyltransferase from Arabidopsis thaliana involved in biosynthesis of type II arabinogalactan has a role in cell elongation during seedling growth', Plant J, 76: 1016-29.
Pubmed: Author and Title
CrossRef: Author and Title
Google Scholar: Author Only Title Only Author and Title

Kotake, T., S. Kaneko, A. Kubomoto, M. A. Haque, H. Kobayashi, and Y. Tsumuraya. 2004. 'Molecular cloning and expression in Escherichia coli of a Trichoderma viride endo-beta-(1-->6)-galactanase gene', Biochem J, 377: 749-55.
Pubmed: Author and Title
CrossRef: Author and Title
Google Scholar: Author Only Title Only Author and Title

Lee, K. J., B. J. Dekkers, T. Steinbrecher, C. T. Walsh, A. Bacic, L. Bentsink, G. Leubner-Metzger, and J. P. Knox. 2012. 'Distinct cell wall architectures in seed endosperms in representatives of the Brassicaceae and Solanaceae', Plant Physiol, 160: 1551-66.
Pubmed: Author and Title
CrossRef: Author and Title
Google Scholar: Author Only Title Only Author and Title

Loque, D., H. V. Scheller, and M. Pauly. 2015. 'Engineering of plant cell walls for enhanced biofuel production', Current Opinion in Plant Biology, 25: 151-61.
Pubmed: Author and Title
CrossRef: Author and Title
Google Scholar: Author Only Title Only Author and Title

Marcus, S. E., A. W. Blake, T. A. S. Benians, K. J. D. Lee, C. Poyser, L. Donaldson, O. Leroux, A. Rogowski, H. L. Petersen, A. Boraston,

H. J. Gilbert, W. G. T. Willats, and J. P. Knox. 2010. 'Restricted access of proteins to mannan polysaccharides in intact plant cell walls', Plant Journal, 64: 191-203.
Pubmed: Author and Title
CrossRef: Author and Title
Google Scholar: Author Only Title Only Author and Title

Marcus, S. E., Y. Verhertbruggen, C. Herve, J. J. Ordaz-Ortiz, V. Farkas, H. L. Pedersen, W. G. T. Willats, and J. P. Knox. 2008. 'Pectic homogalacturonan masks abundant sets of xyloglucan epitopes in plant cell walls', Bmc Plant Biology, 8.

McCartney, L., S. E. Marcus, and J. P. Knox. 2005. 'Monoclonal antibodies to plant cell wall xylans and arabinoxylans', J Histochem Cytochem, 53: 543-6.
Pubmed: Author and Title
CrossRef: Author and Title
Google Scholar: Author Only Title Only Author and Title

McCleary, B. V., V. A. McKie, A. Draga, E. Rooney, D. Mangan, and J. Larkin. 2015. 'Hydrolysis of wheat flour arabinoxylan, acid-debranched wheat flour arabinoxylan and arabino-xylo-oligosaccharides by beta-xylanase, alpha-L-arabinofuranosidase and beta-xylosidase', Carbohydr Res, 407: 79-96.
Pubmed: Author and Title
CrossRef: Author and Title
Google Scholar: Author Only Title Only Author and Title

Meikle, P. J., N. J. Hoogenraad, I. Bonig, A. E. Clarke, and B. A. Stone. 1994. 'A (1-->3,1-->4)-beta-glucan-specific monoclonal antibody and its use in the quantitation and immunocytochemical location of (1-->3,1-->4)-beta-glucans', Plant J, 5: 1-9.
Pubmed: Author and Title
CrossRef: Author and Title
Google Scholar: Author Only Title Only Author and Title

Pacheco-Villalobos, D., S. M. Diaz-Moreno, A. van der Schuren, T. Tamaki, Y. H. Kang, B. Gujas, O. Novak, N. Jaspert, Z. Li, S. Wolf, C. Oecking, K. Ljung, V. Bulone, and C. S. Hardtke. 2016. 'The Effects of High Steady State Auxin Levels on Root Cell Elongation in Brachypodium', Plant Cell, 28: 1009-24.
Pubmed: Author and Title
CrossRef: Author and Title
Google Scholar: Author Only Title Only Author and Title

Pattathil, S., U. Avci, D. Baldwin, A. G. Swennes, J. A. McGill, Z. Popper, T. Bootten, A. Albert, R. H. Davis, C. Chennareddy, R. Dong, B. O'Shea, R. Rossi, C. Leoff, G. Freshour, R. Narra, M. O'Neil, W. S. York, and M. G. Hahn. 2010. 'A comprehensive toolkit of plant cell wall glycan-directed monoclonal antibodies', Plant Physiol, 153: 514-25.
Pubmed: Author and Title
CrossRef: Author and Title
Google Scholar: Author Only Title Only Author and Title

Pauly, M., and K. Keegstra. 2010. 'Plant cell wall polymers as precursors for biofuels', Curr Opin Plant Biol, 13: 305-12.
Pubmed: Author and Title
CrossRef: Author and Title
Google Scholar: Author Only Title Only Author and Title

Pedersen, H. L., J. U. Fangel, B. McCleary, C. Ruzanski, M. G. Rydahl, M. C. Ralet, V. Farkas, L. von Schantz, S. E. Marcus, M. C. Andersen, R. Field, M. Ohlin, J. P. Knox, M. H. Clausen, and W. G. Willats. 2012. 'Versatile high resolution oligosaccharide microarrays for plant glycobiology and cell wall research', J Biol Chem, 287: 39429-38.
Pubmed: Author and Title
CrossRef: Author and Title
Google Scholar: Author Only Title Only Author and Title

Pettolino, F. A., C. Walsh, G. B. Fincher, and A. Bacic. 2012. 'Determining the polysaccharide composition of plant cell walls', Nature Protocols, 7: 1590-607.
Pubmed: Author and Title
CrossRef: Author and Title
Google Scholar: Author Only Title Only Author and Title

Puhlmann, J., E. Bucheli, M. J. Swain, N. Dunning, P. Albersheim, A. G. Darvill, and M. G. Hahn. 1994. 'Generation of monoclonal antibodies against plant cell-wall polysaccharides. I. Characterization of a monoclonal antibody to a terminal alpha-(1-->2)-linked fucosyl-containing epitope', Plant Physiol, 104: 699-710.
Pubmed: Author and Title
CrossRef: Author and Title
Google Scholar: Author Only Title Only Author and Title

Ralet, M. C., O. Tranquet, D. Poulain, A. Moise, and F. Guillon. 2010. 'Monoclonal antibodies to rhamnogalacturonan I backbone', Planta, 231: 1373-83.
Pubmed: Author and Title
CrossRef: Author and Title
Google Scholar: Author Only Title Only Author and Title

Rillahan, C. D., and J. C. Paulson. 2011. 'Glycan microarrays for decoding the glycome', Annu Rev Biochem, 80: 797-823.
Pubmed: Author and Title

CrossRef: Author and Title
Google Scholar: Author Only Title Only Author and Title

Schmidt, D., F. Schuhmacher, A. Geissner, P. H. Seeberger, and F. Pfrengle. 2015. 'Automated synthesis of arabinoxylan-oligosaccharides enables characterization of antibodies that recognize plant cell wall glycans', Chemistry, 21: 5709-13.
Pubmed: Author and Title
CrossRef: Author and Title
Google Scholar: Author Only Title Only Author and Title

Senf, D., C. Ruprecht, G. de Kruijff, S. Simonetti, F. Schuhmacher, P. Seeberger, and F. Pfrengle. 2017. 'Active Site-Mapping of Xylan-Deconstructing Enzymes with Arabinoxylan Oligosaccharides Produced by Automated Glycan Assembly', Chemistry, 13, 3197-3205.
Pubmed: Author and Title
CrossRef: Author and Title
Google Scholar: Author Only Title Only Author and Title

Smallwood, M., E. A. Yates, W. G. T. Willats, H. Martin, and J. P. Knox. 1996. 'Immunochemical comparison of membrane-associated and secreted arabinogalactan-proteins in rice and carrot', Planta, 198: 452-59.
Pubmed: Author and Title
CrossRef: Author and Title
Google Scholar: Author Only Title Only Author and Title

Steffan, W., P. Kovac, P. Albersheim, A. G. Darvill, and M. G. Hahn. 1995. 'Characterization of a monoclonal antibody that recognizes an arabinosylated (1-->6)-beta-D-galactan epitope in plant complex carbohydrates', Carbohydr Res, 275: 295-307.
Pubmed: Author and Title
CrossRef: Author and Title
Google Scholar: Author Only Title Only Author and Title

Verhertbruggen, Y., S. E. Marcus, A. Haeger, R. Verhoef, H. A. Schols, B. V. McCleary, L. McKee, H. J. Gilbert, and J. P. Knox. 2009. 'Developmental complexity of arabinan polysaccharides and their processing in plant cell walls', Plant J, 59: 413-25.
Pubmed: Author and Title
CrossRef: Author and Title
Google Scholar: Author Only Title Only Author and Title

Vidal-Melgosa, S., H. L. Pedersen, J. Schuckel, G. Arnal, C. Dumon, D. B. Amby, R. N. Monrad, B. Westereng, and W. G. Willats. 2015. 'A new versatile microarray-based method for high throughput screening of carbohydrate-active enzymes', J Biol Chem, 290: 9020-36.
Pubmed: Author and Title
CrossRef: Author and Title
Google Scholar: Author Only Title Only Author and Title

Walker, J. A., S. Pattathil, L. F. Bergeman, E. T. Beebe, K. Deng, M. Mirzai, T. R. Northen, M. G. Hahn, and B. G. Fox. 2017. 'Determination of glycoside hydrolase specificities during hydrolysis of plant cell walls using glycome profiling', Biotechnol Biofuels, 10: 31.
Pubmed: Author and Title
CrossRef: Author and Title
Google Scholar: Author Only Title Only Author and Title

Willats, W. G., S. E. Marcus, and J. P. Knox. 1998. 'Generation of monoclonal antibody specific to (1-->5)-alpha-L-arabinan', Carbohydr Res, 308: 149-52.
Pubmed: Author and Title
CrossRef: Author and Title
Google Scholar: Author Only Title Only Author and Title

Zakharova, A. N., R. Madsen, and M. H. Clausen. 2013. 'Synthesis of a backbone hexasaccharide fragment of the pectic polysaccharide rhamnogalacturonan I', Org Lett, 15: 1826-9.
Pubmed: Author and Title
CrossRef: Author and Title
Google Scholar: Author Only Title Only Author and Title